Mutations in β-Spectrin Disrupt Axon Outgrowth and Sarcomere Structure

Marc Hammarlund, Warren S. Davis, and Erik M. Jorgensen

Department of Biology, University of Utah, Salt Lake City, Utah 84112-0840

Abstract. β-Spectrin is a major component of the membrane skeleton, a structure found at the plasma membrane of most animal cells. β-Spectrin and the membrane skeleton have been proposed to stabilize cell membranes, generate cell polarity, or localize specific membrane proteins. We demonstrate that the *Caenorhabditis elegans* homologue of β-spectrin is encoded by the *unc-70* gene. *unc-70* null mutants develop slowly, and the adults are paralyzed and dumpy. However, the membrane integrity is not impaired in *unc-70* animals, nor is cell polarity affected. Thus, β-spectrin is not essential for general membrane integrity or for cell polarity. However, β-spectrin is required for a subset of processes at cell membranes. In neurons, the loss of β-spectrin leads to abnormal axon outgrowth. In muscles, a loss of β-spectrin leads to disorganization of the myofilament lattice, discontinuities in the dense bodies, and a reduction or loss of the sarcoplasmic reticulum. These defects are consistent with β-spectrin function in anchoring proteins at cell membranes.

Key words: *unc-70* • *Caenorhabditis elegans* • cytoskeleton • neurons • muscles

Introduction

β-Spectrin is an essential component of the membrane skeleton, a dense protein mesh that is associated with the intracellular surface of plasma membranes. The membrane skeleton is primarily formed from $\alpha_2\beta_2$ spectrin tetramers, each composed of two α-spectrin and two β-spectrin subunits (for reviews see Bennett, 1990; Bennett and Gilligan, 1993). Each spectrin subunit is a long, rod-shaped protein consisting mainly of tandem triple helical spectrin repeats (Yan et al., 1993). α-Spectrin has 21 spectrin repeats, an SH3 domain, and a COOH-terminal EF hand, whereas β-spectrin has 17 spectrin repeats, an NH_2-terminal actin-binding domain, and a COOH-terminal pleckstrin homology (PH)[1] domain. $\alpha_2\beta_2$ spectrin tetramers nucleate around short actin filaments to form the membrane skeleton. The membrane skeleton is linked to the plasma membrane by direct interactions between the PH domain in β-spectrin and membrane phospholipids (Davis and Bennett, 1994) and indirect interactions between β-spectrin and integral membrane proteins via the linker protein ankyrin (Bennett and Stenbuck, 1979). Since association of the membrane skeleton with plasma membranes is mediated by β-spectrin, membrane skeleton function at plasma membranes requires β-spectrin.

Spectrin was first identified in erythrocytes (for review see Lux and Palek, 1995). In these cells, detergent extraction leaves behind a ghost, which is a dense protein mesh that follows the contours of the plasma membrane. Erythrocytes are resilient cells that are capable of withstanding high shear forces caused by squeezing through narrow capillaries. Mutations in human erythrocyte spectrin genes cause hereditary anemias, and the erythrocytes from these patients are fragile and exhibit membrane defects such as herniation. These data indicate that β-spectrin and the membrane skeleton control the shape and elasticity of erythrocyte plasma membranes.

More recently, α- and β-spectrins have been found in most metazoan cells and tissue types that have been examined, including most nonerythrocyte tissues of vertebrates. In particular, nonerythrocyte spectrins are abundant in neurons, muscle, and polarized epithelial cells. Two genes for α-spectrin and three for β-spectrin have been identified to date in both mice and humans, each of which is alternatively spliced to produce multiple spectrin isoforms (for review see Morrow et al., 1997). The expression of isoforms is regulated in a complex, tissue- and time-specific manner in a variety of cells. Additionally, spectrin isoforms are not evenly distributed at the plasma membrane, as observed in erythrocytes. For example, in skeletal muscle, spectrin is localized to the Z and M lines, which are the myofilament attachment structures for actin and myosin,

Address correspondence to Erik M. Jorgensen, Department of Biology, University of Utah, 257 South 1400 East, Salt Lake City, UT 84112-0840. Tel.: (801) 585-3517. Fax: (801) 581-4668. E-mail: jorgensen@biology.utah.edu

[1]*Abbreviations used in this paper:* GFP, green fluorescent protein; ORF, open reading frame; PH, pleckstrin homology.

respectively (Porter et al., 1992; Zhou et al., 1998). In cultured MDCK epithelial cells, β-spectrin is associated with the basolateral domain and not the apical domain (Nelson and Veshnock, 1986). This uneven distribution of spectrin isoforms suggests that the membrane skeleton is performing specialized functions at specific regions of the plasma membrane rather than playing a general role in membrane elasticity.

Invertebrates also have a membrane skeleton. *Caenorhabditis elegans* has single genes for α-spectrin (Norman, K., and D. Moerman, personal communication) and β-spectrin (this work), and also a gene for β_H-spectrin, which is a very large spectrin with limited expression (McKeown et al., 1998). The *Drosophila* genome also contains single genes for α- and β-spectrin (Adams et al., 2000) as well as for β_H-spectrin (Thomas et al., 1998). Data from these organisms suggest that their membrane skeleton is functionally similar to that of vertebrates. Most strikingly, the distribution of β-spectrins in *C. elegans* closely parallels the distribution of vertebrate β-spectrin (Moorthy et al., 2000 [this issue]). For example, *C. elegans* β-spectrin is polarized to the basolateral domain in the gut epithelium, and is concentrated at the myofilament attachment structures in muscle.

These results support three models for the role of the membrane skeleton in both vertebrates and invertebrates (Lee et al., 1997). First, the spectrin-based membrane skeleton might function to maintain cell shape and membrane integrity, as proposed for erythrocytes (Lux and Palek, 1995). Second, the membrane skeleton might function to recruit or stabilize interacting proteins to specific regions of the cell membrane (Morrow et al., 1997). Third, the membrane skeleton might play a role in the generation or maintenance of cell polarity (for review see Drubin and Nelson, 1996).

One way to distinguish among these models is to analyze defects found in mutants lacking spectrin. In the present work, we characterize the *unc-70* locus, which encodes the *C. elegans* homologue of β-spectrin. *unc-70* is the first mutation characterized in any species in nonerythrocyte β-spectrin. The first mutant alleles of *unc-70* to be identified were dominant mutations that caused an uncoordinated phenotype (Brenner, 1974; Park and Horvitz, 1986). Recessive lethal alleles of the *unc-70* locus were obtained by reversion of the dominant alleles (Park and Horvitz, 1986), in a screen for lethal mutations (Johnsen and Baillie, 1991), and in a screen for *smg*-dependent dominant mutations (Cali and Anderson, 1998). These recessive alleles were originally reported to be lethal mutations, however, we discovered that under certain conditions, animals homozygous for null mutations in *unc-70* can survive and reproduce. These conditions enabled the study of animals that completely lack β-spectrin. We found that a loss of β-spectrin does not cause general membrane or cell polarity defects in the tissues in which it is normally expressed. Rather, a loss of β-spectrin results in specific defects that depend on the cell type examined. For example, we observed axon outgrowth defects in neurons and myofilament lattice disorganization in muscles. These data suggest that β-spectrin functions differently in different cells, and support a model in which the nonerythrocyte membrane skeleton acts to recruit or stabilize components of specific subcellular processes.

Materials and Methods

Strains and Genetics

Strains were grown at room temperature and maintained as described (Brenner, 1974). *unc-70* null mutants are subviable and are usually maintained as balanced heterozygotes. We found that we could maintain homozygous *unc-70* animals by growing them on fresh plates seeded with HB101 and transferring them every 2 or 3 d. The following strains were used: MT2590, *+/eT1; dpy-11(e224) unc-70(n493n1171)/eT1* (Park and Horvitz, 1986), EG1494: *+/eT1; unc-70(r974)/eT1, EG1988: +/eT1; unc-70(s1502)/eT1*, and EG1989: *+/eT1; unc-70(s1639)/eT1*. EG1494 was constructed from strain TR1848: *smg-1(r861); unc-70(r974)/+* (Cali and Anderson, 1998), EG1988 was constructed from strain BC2303: *dpy-18(e364)/eT1; unc-46(e177) unc-70(s1502)/eT1* (Johnsen and Baillie, 1991), and EG1989 was constructed from strain BC2440: *dpy-18(e364)/eT1; unc-46(e177) unc-70(s1639)/eT1* (Johnsen and Baillie, 1991).

Genetic Mapping

unc-70 was previously mapped to chromosome V (Brenner, 1974) to the right of *dpy-11* (Park and Horvitz, 1986) and to the left of *unc-68*. We mapped *unc-70(n493n1171)* to the interval between *snb-1* and *unc-68*. From the progeny of *dpy-11(e224) unc-70(n493n1171)/snb-1(md247)*, we isolated nine Dpy non-Unc animals. Four of these nine animals segregated the *snb-1* phenotype, indicating that *unc-70* is to the right of *snb-1*.

unc-70 Rescue

Cosmids from the *snb-1* to *unc-68* interval were injected into MT2590 and scored for rescue of *unc-70*. The cosmid T19F4 was capable of complete rescue. To identify the open reading frame (ORF) corresponding to *unc-70*, individual ORFs from the T19F4 cosmid were amplified using the Expand Long Template PCR system (Boehringer Mannheim); the fragments were gel-purified and recovered using a QIAquick column (Qiagen), injected into MT2590, and assayed for rescue. A 12.9-kb PCR product containing the spectrin ORF was capable of complete rescue. This fragment extended 2.6 kb, 5′ of the predicted start, and 1.3 kb, 3′ of the predicted stop. All injections were performed essentially as described (Mello et al., 1991). Injection mixtures for the rescue contained either 20 ng/μl T19F4 cosmid or 20 ng/μl purified PCR product, together with 60 ng/μl of the plasmid pRF4, which contains the dominant roller mutation *rol-6(su1006)*, as a transformation marker (Mello et al., 1991). For both T19F4 and PCR fragment rescue, three of three stable roller lines rescued the mutant phenotype.

cDNA Sequence

Most of the *unc-70* cDNA sequence was obtained by spliced leader sequence PCR (Krause, 1995) and reverse transcriptase–PCR. For these experiments, the total *C. elegans* RNA was prepared essentially as described (Andres and Thummel, 1994). Reverse transcription and PCR were performed by standard methods using the following primer sets, which yielded a sequence extending from the SL-splice in exon 1 through the 3′ end of exon 7: RT: MH143, PCR: SL1 and MH144; RT: MH141, PCR: MH106 and MH142, MH103 and MH104; RT: MH138, PCR: MH139 and MH140, MH107 and MH108; and RT: MH137, PCR: MH113 and MH114, MH111 and MH112. PCR products were purified and all bands were sequenced. These experiments yielded the CeβS1 isoform; no alternative splicing was detected. However, the results from Genefinder predictions (Baylor College of Medicine) suggested that there might be alternative exon usage. Therefore, we repeated this experiment using the following primer set: RT: MH143, PCR: MH163 and MH144. A second isoform was detected corresponding to CeβS2.

The remaining cDNA sequence 3′ of exon 7 was obtained in two ways. First, a cDNA library obtained from P. Okkema (University of Illinois at Chicago, Chicago, IL) was probed with a 10.4-kb EcoRI-SpeI genomic fragment from T19F4, and one clone was isolated. Second, two cDNA clones corresponding to *unc-70*, yk144e2, and yk164c6, were obtained from Y. Kohara (Genome Biology Lab, National Institute of Genetics, Mishima, Japan). All three clones were completely sequenced and no alternative splicing was detected. The Okkema clone contained a poly(A)$^+$ sequence downstream of a strong consensus polyadenylation signal. Sequence alignments were performed with ClustalW (Thompson et al., 1994).

unc-70 Mutant Sequence

For each allele, the overlapping fragments covering the entire *unc-70* genomic region were amplified from homozygous *unc-70* animals. The sequences of all exons were determined using an Applied Biosystems automated DNA sequencing apparatus at the Sequencing Core Facility (University of Utah).

unc-70::GFP Reporters

To determine in which cells the two *unc-70* splice variants (CeβS1 and CeβS2) are expressed, we used reporter constructs expressing green fluorescent protein (GFP; Chalfie et al., 1994). Reporter constructs, including a 4-kb construct upstream of the predicted ATG codon, were prepared by amplifying fragments from the T19F4 cosmid using the Expand Long Template PCR system (Boehringer Mannheim); primers were tagged with a PstI site at the 5′ end and an SacI site at the 3′ end. These fragments were cloned into the pPD95.67 GFP vector (1995 Fire vector kit) in the PstI-SacI sites. The resulting constructs contain the *unc-70* promoter and differing lengths of *unc-70* coding sequence in-frame with the nuclear localization sequence and GFP.

For CeβS1 expression, we fused the GFP ORF to the second exon of *unc-70* (CeβS1::GFP). Conceptual translation of CeβS1::GFP predicts that it encodes the 22 NH_2-terminal amino acids of CeβS1 linked to GFP. For CeβS2 expression, we fused the GFP ORF to the first in-frame ATG in the third exon of *unc-70* (CeβS2::GFP). We also fused GFP to exons 4, 5, and 6, which are common to both CeβS1 and CeβS2. GFP expression from exons 4, 5, and 6 was identical to CeβS1::GFP. These constructs are not expressed in the gut, even though they should include expression from the CeβS2 splice form. However, gut expression has been verified by immunofluorescence (Moorthy et al., 2000 [this issue]).

Primer pairs used for construction of GFP fusions were as follows: for CeβS1::GFP, MH149 and MH148; for CeβS2::GFP, MH123 and MH122; for exon5::GFP, MH149 and MH147; for exon6::GFP, MH149 and MH180; and for exon4::GFP, MH149 and MH182. Each construct was injected at 20 ng/μl into *lin-15(n765ts)* animals, together with the *lin-15*(+) plasmid pEK1 (Clark et al., 1994) as an injection marker. At least three stable *lin-15*(+) lines were obtained for each construct; in all cases, lines had similar expression patterns.

Neuron and Muscle Staining

The GABA nervous system was visualized using the reporter construct *oxIs12* (McIntire et al., 1997). *oxIs12* expresses GFP under the control of the promoter for the vesicular GABA transporter gene *unc-47*. We crossed *oxIs12* animals to *unc-70(s1639)/+* and *unc-70(s1502)/+* animals and obtained animals heterozygous for both *unc-70* and *oxIs12*. From these animals, we isolated homozygous *unc-70* animals expressing GFP, and photographed the progeny of these homozygous animals.

For muscle staining, progeny of homozygous *unc-70(s1639)* and *unc-70(s1502)* animals were collected and stained with the antiparamyosin mAb NE8/4C6.3 (Goh and Bogaert, 1991) by the whole-mount fixation method essentially as previously described (Miller and Shakes, 1995). Confocal images were collected and assembled with LaserSharp2000 (Bio-Rad Microscience Ltd., Hemel Hempstead, UK). The results were consistent among alleles; images are of representative animals.

Electron Microscopy

Adult progeny of homozygous *unc-70(s1639)*, *unc-70(s1502)*, and *unc-70(r974)* hermaphrodites were prepared for electron microscopy as previously described (Richmond et al., 1999). Ribbons of ultrathin sections (~35 nm) were collected and examined on a Hitachi H-7100 transmission electron microscope (Hitachi Ltd.) equipped with a Gatan slow-scan digital camera (Gatan, Inc.). Images were adjusted for brightness, contrast, and size with Adobe Photoshop 5.0. Morphometry was analyzed using the public domain software package NIH Image.

For quantification of the synaptic vesicle number and localization, we examined 500 serial sections from two animals of the wild type, 650 sections from three animals of *unc-70(s1639)*, and 100 sections from two animals of *unc-70(s1502)*. A synapse was defined as all adjacent serial sections containing a higher than average number of vesicles surrounding a presynaptic density. To obtain the percentage of vesicles found at the plasma membrane, we counted all vesicles in each synapse that were touching or within one vesicle diameter of the plasma membrane, divided by the total number of vesicles per synapse. Similar percentages were obtained by counting only vesicles that were touching the plasma membrane (data not shown). To obtain the percentage of vesicles found at the presynaptic density, we counted all vesicles that were touching or within one vesicle diameter of the presynaptic specialization, divided by the total number of vesicles per synapse.

Statistical Analysis

Data were analyzed using InStat for Macintosh version 2.03 (Graphpad software). An unpaired *t* test was used to compare data sets and a two-tailed *P* value was calculated.

Primer Sequences

MH103 attcttgcgcaatcaacacg; MH104 tgttcgagtttctcttgacg; MH106 agcttgttgatgtaatcacg; MH107 attgcaagatgaaagcatcc; MH108 cttgatatcttcacgaatgg; MH111 agatgagacttacagagacg; MH112 gttcgtgtttcttgatttgg; MH113 attgtacatgatgcaagacg; MH114 agttcatttctctcttcacc; MH120 gtcagggtcacttggaaaccaatt; MH121 gttggcttagtcggttagaaagag; MH122 ctgcagctggtgctgatttgtgttt; MH123 gagctctgtaaagagaatgcacaag; MH137 ttctcgatttcacttgatgcgtagt; MH138 aacaacttctgtcccttctcctctgta; MH139 atggttccgtggtactctggc; MH140 aagattgtccatgatggaacgc; MH141 gcggagagtatcatacaagtagcgat; MH142 tgagaaggcagaacacgaacg; MH143 agcagttttcatctggcaccac; MH144 agatgagacccaacgtgaggc; MH147 gagctcacgagttcacgttcatctg; MH148 gagctcgacgagttgtcatcatagtc; MH149 ctgcagtctcctctctttcgcttc; MH163 atgacgagcatcatccttc; MH180 gagctcaggagcatttttccgtctcgc; MH182 ggctcgagcctctgaacctcaagtcaac; and SL1 ggtttaattacccaagtttgag.

Results

Molecular Characterization of unc-70

Recessive *unc-70* mutants are shorter than the wild type, are paralyzed, and are nearly inviable (Fig. 1). To determine the protein encoded by *unc-70*, we characterized the gene. We mapped *unc*-70 to a narrow interval flanked by *snb-1* and *unc-68* on chromosome V (Fig. 2 A). We injected cosmids from the region between *snb-1* and *unc-68* and obtained the complete rescue of *unc-70(n493n1171)* with the single cosmid T19F4. A 12.9-kb region of this cosmid containing a single predicted ORF was amplified using PCR and was capable of completely rescuing *unc-70(n493n1170)* (Fig. 2 B).

Analysis of the rescuing ORF indicated that *unc-70* encodes a *C. elegans* homologue of vertebrate β-spectrin (Fig. 3). We determined the structure of the *unc-70* mRNA by examining cDNAs isolated by spliced leader sequence PCR, reverse transcription PCR, and from cDNA libraries. These experiments identified two splice variants of the *unc-70* gene that differ only at their NH_2 termini (Fig. 2 C). We refer to the predicted products of these splice vari-

Figure 1. Light microscope images of (A) wild-type and (B) *unc-70(r974)* adult animals.

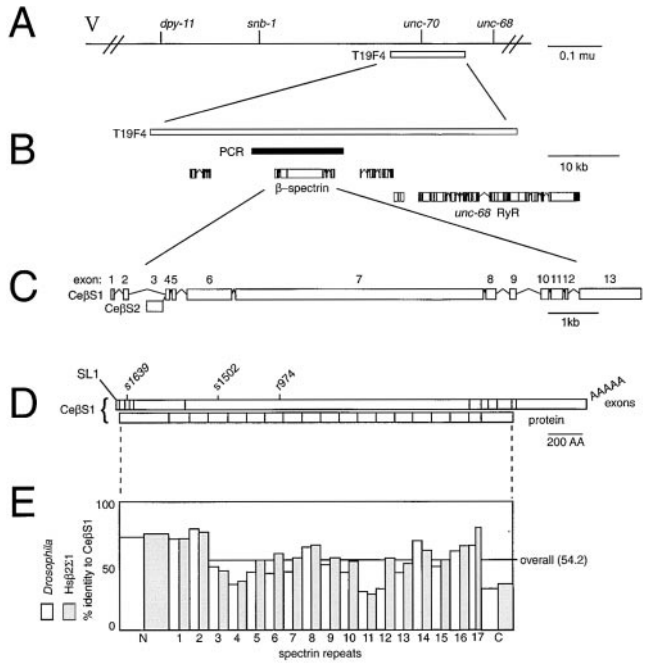

Figure 2. Genetic and molecular characterization of *unc-70*. (A) Genetic map of the *unc-70* region. (B) Rescue of *unc-70*. The cosmid T19F4 rescued the *unc-70* phenotype in three out of three lines. An 11.9-kb PCR fragment, only containing the spectrin gene, also rescued the *unc-70* phenotype in three out of three lines. Predicted ORFs are shown below. (C) *unc-70* cDNAs. Exons are shown as closed boxes and introns as lines. Two splice variants, CeβS1 and CeβS2, are shown. CeβS1 is trans-spliced to the SL1 sequence. The 5′ end of CeβS2 was not determined. (D) cDNA and protein structure comparison. (top) CeβS1 cDNA showing the exon boundaries and the positions of three nonsense alleles induced by ethylmethane sulfonate. *unc-70(s1639)* is a G to A transition that changes Trp49 to a UAG codon; *unc-70(s1502)* is a C to T transition that changes Gln576 to a UAA codon; and *unc-70(r974)* is a G to A transition that changes Trp927 to a UGA codon. (bottom) Domains of the protein. (E) Domain-by-domain comparison of the percent identity between CeβS1, Hsβ2S1, and *Drosophila* β-spectrin. The NH_2-terminal domain, spectrin repeats, and COOH-terminal domains are indicated below.

ants as CeβS1 and CeβS2 in accordance with the standard spectrin terminology. Both variants are predicted to encode proteins containing all of the canonical β-spectrin domains, including an NH_2-terminal actin-binding region, a central region containing 17 spectrin repeats, and a COOH-terminal PH domain. All of the spectrin repeats except the 1st and the partial 17th repeat are contained within a single, very large exon (Fig. 2 D). The functional significance of this gene structure is not known, and is not observed in the two other known *C. elegans* spectrins, β_H-spectrin (McKeown et al., 1998), and α-spectrin (Moerman, D., personal communication).

CeβS1 is predicted to contain 2,257 residues (~262 kD) and is 54.2% identical to human β2Σ1 spectrin, which is the major nonerythrocyte β-spectrin isoform in vertebrates (Hu et al., 1992; Figs. 2 E and 3). The *C. elegans* genome sequence is essentially complete (*C. elegans* Sequencing Consortium, 1998), and BLAST searches failed to identify any other β-spectrin homologues (Altschul et al., 1997). Thus, *unc-70* is likely to encode the only *C. elegans* β-spectrin. We compared individual domains of CeβS1 to human β2Σ1 and to *Drosophila* β-spectrin to identify strongly conserved regions and found four such regions (Fig. 2 E). The first includes the NH_2-terminal actin-binding domain and the first two spectrin repeats that nucleate αβ heterodimer formation and interact with adducin and other proteins. The second and third regions of conservation are centered on the 8th and 14th spectrin repeats, respectively; no specific functions have been previously localized to these repeats. Finally, the fourth region of conservation encompasses the last two spectrin repeats, which are essential for the formation of $\alpha_2\beta_2$ spectrin tetramers (Kennedy et al., 1994).

Expression of unc-70

The severe uncoordinated phenotype of *unc-70* suggested that *unc-70* was likely to be expressed in the motor system, either in muscles or neurons. We determined the expression pattern of the *unc-70* gene using GFP reporter constructs. GFP expression for the predominant isoform (CeβS1::GFP, see Materials and Methods) was first detected in the embryo in all cells except the intestine; by hatching, expression was confined mainly to neurons and muscles. In the adult, the strongest expression was found in neurons, all or nearly all of which expressed this isoform (Fig. 4, A and C). This correlates well with the high levels of UNC-70 protein observed by immunofluorescence in neurons (Moorthy et al., 2000 [this issue]). Robust expression was also observed in all muscles, including the pharyngeal (Fig. 4 A), vulval, uterine, enteric (Fig. 4 B), and the body wall (Fig. 4 C) muscles. Again, UNC-70 protein is found in these cells (Moorthy et al., 2000 [this issue]). The spermatheca also expressed the predominant isoform (Fig. 4 D), and low levels of expression were observed in the hypoderm. The gut and gonad did not express visible levels of the predominant isoform. Expression of the second isoform (CeβS2::GFP; see Materials and Methods) was also detected in embryos, in all larval stages, and in adults. However, expression of this isoform was confined to the gut from at least hatching onwards (Fig. 4, E and F). Expression of the *unc-70* gene in the gut is confirmed by immunofluorescence, which reveals UNC-70 protein in the gut at all developmental stages (Moorthy et al., 2000 [this issue]). Neurons and muscles that expressed high levels of the predominant isoform did not express visible levels of the gut-specific isoform. Together, these results demonstrated that β-spectrin is expressed in most tissues of *C. elegans* throughout its life span.

unc-70 Mutations

To ensure that the phenotype observed in *unc-70* animals represents the null phenotype for this locus, we identified a molecular null in the *unc-70* gene by sequencing recessive alleles. *unc-70(s1639)* is likely to be a functional and a molecular null for three reasons. First, the mutation introduces a stop codon that truncates the predicted protein after 48 residues and, therefore, lacks all of the functional domains of the β-spectrin. This mutation is in an exon

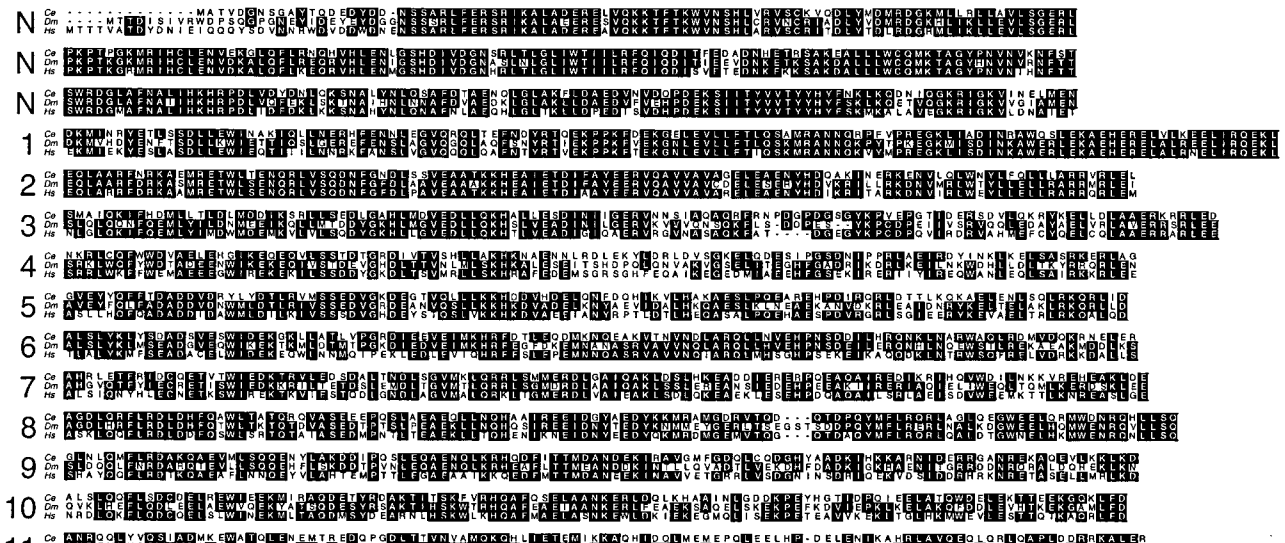

Figure 3. Sequence alignment of the *C. elegans* (*Ce*; GenBank accession number AF261891), *Drosophila* (*Dm*; GenBank accession number AAA28399), and human (*Hs*; GenBank accession number AAA60580) homologues of β-spectrin. Identical residues are in black boxes; numbers indicate spectrin repeats.

common to both the CeβS1 and the CeβS2 isoforms. Second, it is as severe as any other *unc-70* allele; in fact, all alleles are indistinguishable as homozygotes. Third, *unc-70(s1639)* homozygous animals show no immunoreactivity to a β-spectrin antibody (data not shown; antibody provided by S. Moorthy and V. Bennett). We also identified two other alleles, *s1502* and *r974*, that truncate the predicted protein after 575 and 927 residues respectively; these mutations are also in exons common to the two isoforms (Fig. 2 D). We observed no phenotypic differences among these three alleles. Thus, we used these presumptive null alleles to infer the function of β-spectrin.

unc-70 is the only β-spectrin in the *C. elegans* genome. Further, while β_H-spectrin is similar to β-spectrin in some respects, it is unlikely to substitute functionally for the loss of β-spectrin. β_H-Spectrin is expressed primarily during embryogenesis, and is found mainly in epithelial tissues (McKeown et al., 1998). Even in epithelial tissues that express both β-spectrin and β_H-spectrin, these proteins appear to play separate roles since β-spectrin is located at the basolateral membrane, whereas β_H-spectrin is found at the apical membrane (Thomas and Kiehart, 1994). Therefore, null mutations in *unc-70* are likely to result in a complete loss of β-spectrin function.

β-Spectrin Is Not Required for Cell Polarity or Membrane Integrity

One hypothesized role for β-spectrin is that it functions in the generation of cell polarity (Drubin and Nelson, 1996). To test whether the loss of β-spectrin affects cell polarity, we compared the polarized epithelial cells of the *C. elegans* gut in *unc-70(r974)* to those of the wild type (White, 1988). We found no evidence of a loss of polarity in *unc-70(r974)* animals by the ultrastructural criteria (n = 6 worms). Both the apical (Fig. 5, A and C) and the basolateral (Fig. 5, B and D) domains of the intestine were normal in *unc-70(r974)* mutants. Specifically, the microvilli and electron-dense structures underlying the apical membrane were indistinguishable from those of the wild type (Fig. 5, A and C, arrowheads). Belt desmosomes were also present in *unc-70(r974)* (Fig. 5, A and C, arrows). The basolateral membrane of *unc-70(r974)* was also indistinguishable from the wild type (Fig. 5 B and D, arrow). Similar results were found in *unc-70(s1502)* and *unc-70(s1639)*. Together, these results show that β-spectrin is not required for the generation or maintenance of cell polarity in the gut epithelium. To test whether this was true in other tissue types, we examined *unc-70(r974)*, *unc-70(s1502)*, and *unc-70(s1639)* neurons and muscles for cell

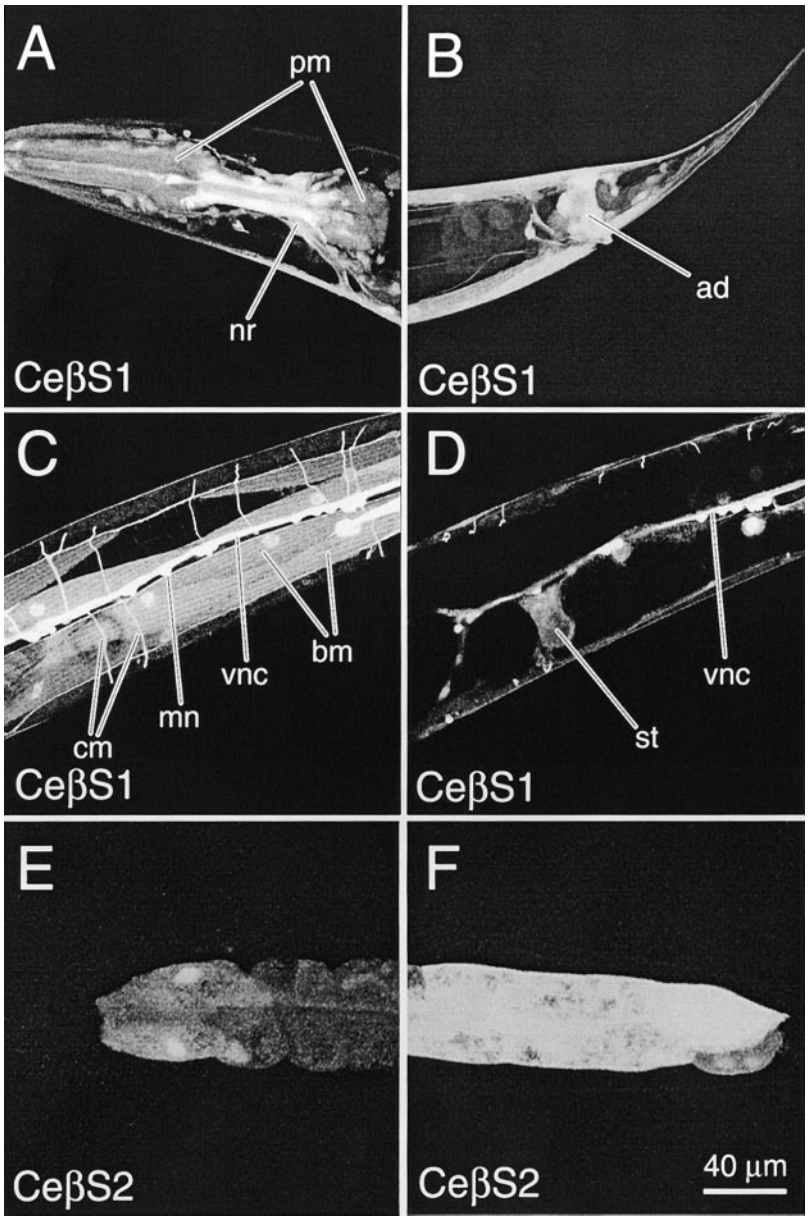

Figure 4. Expression pattern of *unc-70*. Adult animals expressing GFP reporter constructs are oriented anterior to the left and dorsal surface to the top except C and D, which depict the ventral surface. GFP was visualized using confocal fluorescent microscopy. (A–D) CeβS1 isoform expression. (A) Pharyngeal muscles (pm) and nerve ring (nr); (B) anal depressor muscles (ad); (C) body wall muscles (bm), motor neurons (mn), commissures (cm), and ventral nerve cord (vnc); note, there is one trapezoidal muscle cell visible that does not express GFP; and (D) spermatheca (st) and ventral nerve cord (vnc). (E and F) CeβS2 isoform expression. Expression is observed exclusively in the intestine, and is brightest at the anterior (E) and posterior (F).

polarity defects (see below). While both of these tissues exhibited severe defects in *unc-70* mutants, we found no evidence that cell polarity was defective. Thus, β-spectrin is not a general determinant of cell polarity.

β-Spectrin also has been proposed to function in the general membrane integrity (Lux and Palek, 1995). We inspected the plasma membrane of *unc-70(r974)*, *unc-70(s1502)*, and *unc-70(s1639)* for the presence of general membrane defects such as herniation, invagination, vesiculation, or the loss of cell–cell contact. We found no general membrane defects in any of the tissues examined, which included the gut epithelia (Fig. 5), neurons (see Fig. 7), and muscles (see Fig. 9). Thus, neither epithelial cells, neurons, nor muscles rely on β-spectrin to maintain the integrity and shape of their plasma membranes.

β-Spectrin Is Required for Axonal Outgrowth

Animals homozygous for null alleles of *unc-70* exhibit phenotypes, such as paralysis, which could be attributed to abnormal neural function. To assess potential defects in the nervous system of *unc-70* homozygous animals, we visualized the GABA nervous system of wild-type and *unc-70(s1639)* animals using a GFP reporter construct (Fig. 6, A–D). To test whether the lack of β-spectrin affects neurogenesis or neuronal cell differentiation, we assayed whether *unc-70(s1639)* animals have the normal number of GABA neurons. We found that *unc-70(s1639)* does not result in a defect in the number of neurons; all worms examined had the normal complement of 19 GABA motor neurons in the ventral nerve cord ($n = 5$ worms; McIntire et al., 1993). Moreover, while spacing of the neuronal cell bodies is not as regular in *unc-70(s1639)* as in the wild type, in general these cell bodies are positioned along the ventral side of the animal and are distributed along the anterior–posterior axis. Thus, β-spectrin does not appear to play an essential role in neurogenesis, neuronal cell identity, or migration, at least in the GABA

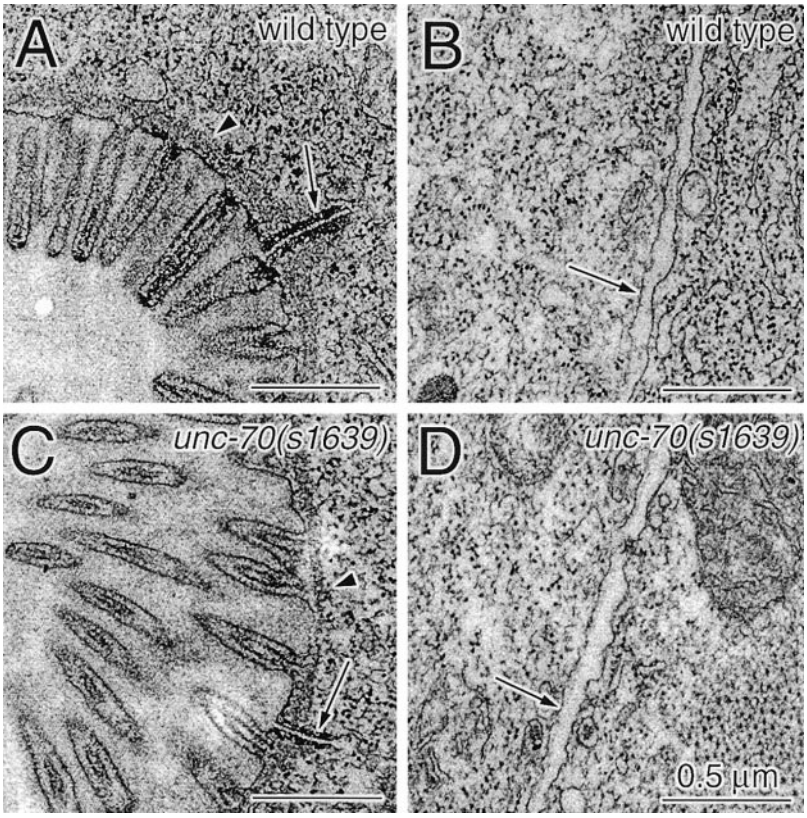

Figure 5. Normal ultrastructure of *unc-70* gut epithelia. Adult wild-type (A and B) and *unc-70(s1639)* (C and D) animals were fixed, and the transverse sections were imaged by transmission electron microscopy. (A and C) Apical membrane. Each panel shows part of two intestinal cells with microvilli extending into the lumen of the gut. (arrows) Belt desmosome; and (arrowheads) electron-dense structures at the apical membrane. (B and D) Basal membrane (arrow).

motor neurons. Similar results were obtained with *unc-70(s1502)*.

To determine the role of β-spectrin in axon outgrowth, we examined three structures in *unc-70* animals: the ventral nerve cord, the commissures that extend from the ventral to the dorsal cord, and the dorsal cord. We found defects in all of these structures, demonstrating that *unc-70* has an important role in axon outgrowth. Specifically, the ventral nerve cords in all *unc-70(s1639)* animals examined (n = 5 worms) were defasciculated, and in most animals, segments of the ventral nerve cord appeared to be composed of a single process (n = 5 worms; Fig. 6 D, arrow).

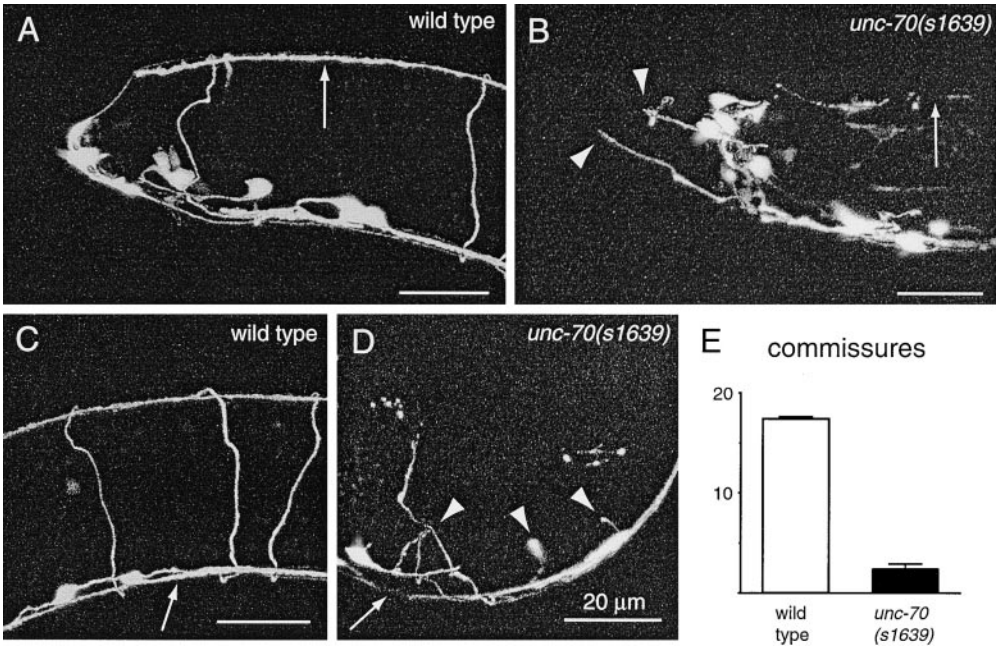

Figure 6. Defects in the morphology of the *unc-70* nervous system. Neurons are visualized using a *unc-47*::GFP construct that expresses GFP in the GABA neurons (McIntire et al., 1997). Adult wild-type (A and C) and *unc-70(s1639)* (B and D) animals are oriented anterior to the left and dorsal surfaces to the top. (A and B) Head region. (arrow) Dorsal cord; and (arrowheads) inappropriate anterior extensions. The dorsal cord in *unc-70* is incomplete. (C and D) Middle region. (arrow) Ventral cord; and (arrowheads) aberrant commissure phenotypes. The ventral cord in *unc-70* is discontinuous and defasciculated. Commissures are either elaborately branched or prematurely terminated. (E) The number of commissures that reached the dorsal cord. Only commissures that reached the dorsal surface were counted. Our analysis may slightly underestimate the number of commissures since the actual number in the wild type is 19 (White et al., 1986).

Despite these defects, however, all animals had regions of their ventral cord that appeared similar to the wild type, suggesting that some axon outgrowth along the ventral cord occurs even in the absence of β-spectrin.

All *unc-70(s1639)* animals examined had severe defects in their commissural outgrowth (Fig. 6 E). Only 2.4 (± 0.5, $n = 5$) commissures reached the dorsal cord in *unc-70(s1639)* animals, compared with 17.4 (± 0.2, $n = 5$; $P < 0.0001$) identified in wild type. The few commissures present in *unc*-70 animals, whether or not they reached the dorsal cord, displayed a variety of aberrant morphologies (Fig. 6 D, arrowheads). Many wandered, were branched, and often gave rise to large, complex elaborations elongated along the anterior–posterior axis. Other commissures terminated prematurely, sometimes ending with a large terminal expansion similar in appearance to a growth cone. We also observed commissures extending anterior of the GABA-expressing RME neurons, where none are normally present (Fig. 6 B, arrowheads).

Compared with these severe defects in commissural outgrowth, outgrowth along the dorsal cord was relatively unaffected. Specifically, of the commissures that reached the dorsal cord in the *unc-70(s1639)* animals, most (7/12 commissures) extended along the anterior–posterior axis to form a short segment of dorsal cord (Fig. 6 B, arrow). Thus, extension along the dorsal cord appears to be more normal (58%, 7/12) than the extension from the ventral to dorsal cord (14%, 12/87) in *unc-70* mutants. Growth cone migration from the ventral to the dorsal cord may be specifically difficult because of the absence of previously formed axons with which a growth cone can fasciculate or because of an increased number of physical obstacles that the growth cone must negotiate (Knobel et al., 1999).

β-Spectrin Is Not Required for Synaptogenesis or Synaptic Vesicle Localization

Because UNC-70 is highly expressed in mature as well as in developing neurons, *C. elegans* β-spectrin could play a role in neuronal function in addition to its requirement during axon outgrowth. To determine whether spectrin is required for the structure of the synapse, we analyzed the ultrastructure of neuromuscular junctions in *unc-70(s1639)* and *unc-70(s1502)* animals. Surprisingly, we found no significant difference between wild-type and *unc-70* animals (Fig. 7, A and B). Neuronal membranes appeared identical in wild-type and *unc-70* animals; as described above, they showed no membrane defects such as herniation, invagination, vesiculation, or loss of cell–cell contact. Presynaptic specializations also appeared normal in *unc-70* animals (arrows).

To identify the potential defects in synaptic vesicle production, localization, release, or endocytosis, we quantified the distribution of synaptic vesicles in *unc-70(s1639)* and wild-type synapses (Fig. 7, C). The average number of synaptic vesicles per synapse did not differ significantly between wild-type and *unc-70(s1639)* animals (wild type = 297 ± 30, $n = 19$; *unc-70(s1639)* = 386 ± 74, $n = 16$; $P = 0.25$). Furthermore, we found no significant difference in the localization of these synaptic vesicles, both for the proportion of the vesicles at the plasma membrane (wild type = 34 ± 3%, $n = 17$; *unc-70(s1639)* = 35 ± 3%, $n = 15$; $P = 0.73$) and for the proportion of vesicles at the presynaptic specialization (wild type = 11 ± 1%; *unc-70(s1639)* = 9 ± 1%; $P = 0.24$). Although these data do not preclude a functional role for spectrin at the synapse, they do suggest that spectrin is not playing a structural role. In addition, the presence of synaptic vesicles and other synaptic components at their normal locations suggests that neuronal cell polarity does not require β-spectrin.

β-Spectrin Is Required for Normal Sarcomere Structure

Because β-spectrin is expressed in muscles at all developmental stages, it is possible that the paralyzed phenotype of *unc-70* mutants is caused in part by the loss of spectrin in muscles. To visualize sarcomere structure, we stained thick filaments using an antibody against paramyosin (Goh and Bogaert, 1991). Because *C. elegans* body wall

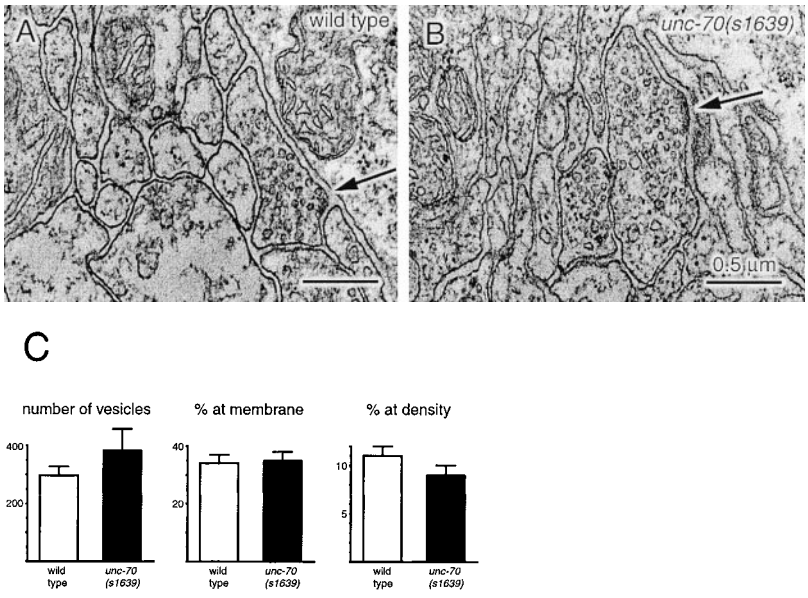

Figure 7. Synaptic ultrastructure is normal at *unc-70* neuromuscular junctions. Sections show a representative GABA neuromuscular junction in the ventral nerve cord of adult wild-type (A) and *unc-70(s1639)* (B) animals. (arrows) Presynaptic density of the synapse. Body wall muscle is shown at the right side in both images. (C) Distribution of synaptic vesicles in the wild type and in *unc-70(s1639)*. *unc-70(s1639)* does not differ significantly from the wild type.

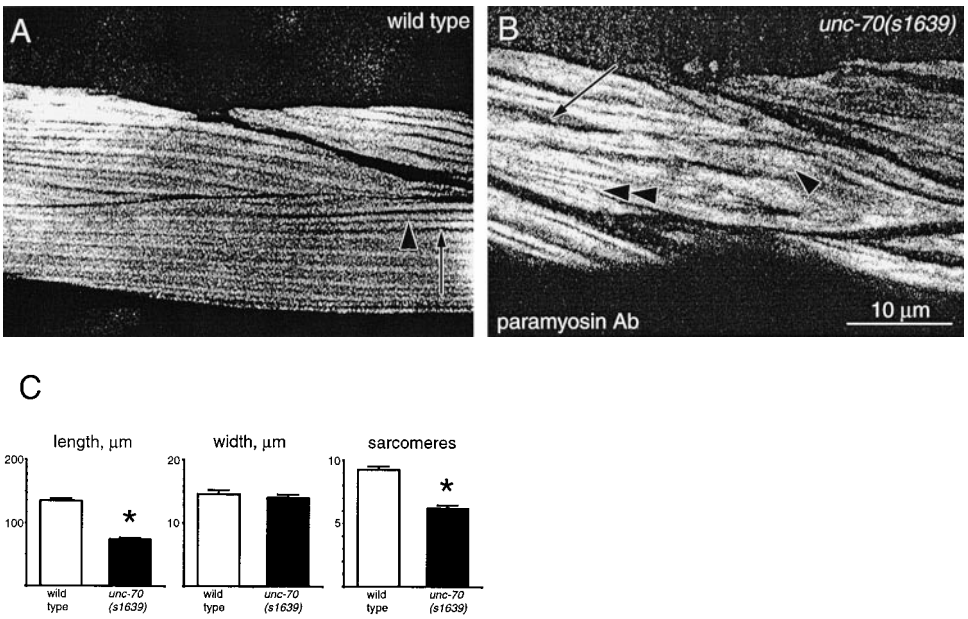

Figure 8. Defects in *unc-70* sarcomere organization. Adult wild-type (A) and *unc-70(s1639)* (B) animals were stained with an antiparamyosin antibody to visualize thick filaments (A bands). In wild-type muscle (Fig. 8 A), thick nonstaining bands (I bands, arrow) alternate with thin nonstaining bands (M line, arrowhead). This regular banding pattern is not present in *unc-70(s1639)*. Both enlarged gaps between A bands (arrow) and overlaps of adjacent A bands (arrowhead) are present. However, despite the disorganization of *unc-70(s1639)* muscle, some areas are similar to the wild type (double arrowhead). (C) Quantification of muscle structure. Asterisk indicates significance ($P < 0.001$).

muscles are obliquely striated, the myosin- and paramyosin-containing thick filaments (A bands) are arranged in regular bands almost parallel to the axis of contraction (Fig. 8 A). These brightly staining bands are separated by thick nonstaining bands, which are the actin-containing thin filaments (I bands, arrow), and by thin nonstaining bands, which are the myosin attachment structures (M lines, arrowhead). To determine whether *unc-70* mutations affect the overall shape of muscle cells, we compared the length and width of these cells to those of the wild type (Fig. 8 C). We found that on average, *unc-70(s1639)* muscles were shorter than wild-type muscles, which is consistent with the short overall body size of the *unc-70* mutants (wild type = 135 ± 3.7 μm, $n = 4$; *unc-70(s1639)* = 74 ± 2.6 μm, $n = 8$; $P < 0.0001$). The width of *unc-70(s1639)* muscles was not significantly different than wild type (wild type = 14.6 ± 0.7 μm, $n = 5$; *unc-70(s1639)* = 14.0 ± 0.5 μm, $n = 9$; $P = 0.5276$). In addition to the reduced length of muscles in the mutants, the arrangement of sarcomeres was disrupted when compared with those of the wild type. Fewer sarcomeres were found in *unc-70(s1639)* muscles than in the wild type (wild type = 9.3 ± 0.3, $n = 4$; *unc-70(s1639)* = 6.2 ± 0.2, $n = 9$; $P < 0.0001$). On average, each *unc-70(s1639)* sarcomere was wider than in the wild type (wild type = 1.57 μm, *unc-70(s1639)* = 2.26 μm). However, it was readily apparent that this average increase in sarcomere width in *unc-70* muscles was unevenly distributed (Fig. 8 B). The width of individual sarcomeres often varied along their length in *unc-70* mutants; variable widths were never observed in the wild type. Further, the relationship between adjacent sarcomeres was disrupted in *unc-70*, such that in some areas, large gaps appeared between A bands (arrow), whereas in other areas, adjacent A bands appeared to overlap (arrowhead). However, most muscles also had small regions in which the banding pattern appeared normal (double arrowhead). These data suggested that *unc-70* is required for normal myofilament organization.

These defects in sarcomere structure were confirmed at the ultrastructural level (Fig. 9). In transverse sections of wild-type specimens, the alternating bands of thick and thin filaments (A and I bands, respectively) were clearly defined. Rarely, we observed *unc-70* sections that lacked thick filaments; these sections likely correspond to the gaps between sarcomeres discussed above. In most *unc-70* sections, a distinct band of thin filaments was not visible; instead, thick filaments were found throughout the section, often clustered around the dense bodies. These phenotypes appear to correspond to the enlargement of brightly staining thick filament–containing areas that we observed with paramyosin staining. In addition to the mislocalization of thick filaments, these filaments were not clustered in evenly spaced columns as they are in the wild type. Finally, M lines were reduced or absent.

In addition to defects in the arrangement of the myofilament lattice, *unc-70* animals had defects in dense body and sarcoplasmic reticulum morphology. Dense bodies in mutant specimens were narrower than the wild type and often were observed to taper sharply, whereas in the wild type, they appeared uniformly thick. Discontinuities in the electron-dense portion of the dense bodies, never observed in the wild type, are often present in *unc-70* muscles (Fig. 9 B, arrow). In the wild type, the sarcoplasmic reticulum is a series of elongated vesicles closely associated with the dense bodies and with the plasma membrane beneath the myofilament lattice (Fig. 9 A, arrowheads). These structures were reduced in number or absent in *unc-70* muscles. When present, their distribution was restricted to the plasma membrane, never extending along the sides of the dense bodies as observed in the wild type.

Despite the severe defects observed in *unc-70* sarcomere organization, the overall muscle organization was normal, with the myofilaments and dense bodies polarized to the hypodermal side of muscle cells. Also, the sarcomeres were correctly oriented parallel to the body axis. This sug-

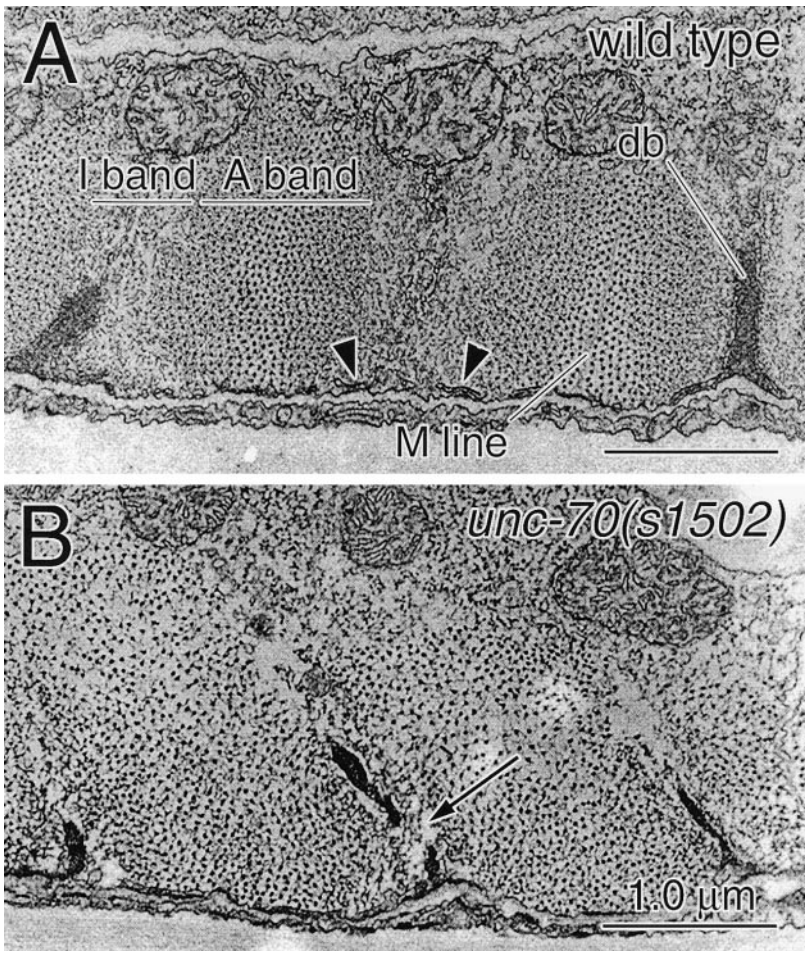

Figure 9. Ultrastructural defects in *unc-70* muscles. Sections show a representative region of the adult wild-type (A) and *unc-70(s1502)* (B) body wall muscle. Each panel shows three dense bodies (db) and the neighboring myofilament lattice; the hypodermis is at the bottom. The I and A bands and the M line are indicated in the wild-type muscle; no similar organization is present in *unc-70(s1502)*. Arrowheads indicate sarcoplasmic reticulum, which is not present in *unc-70* animals.

gests that β-spectrin is not required for overall cell polarity in muscles.

The structural defects seen in *unc-70* muscles could be due to the β-spectrin function in the development of the sarcomeres or to the β-spectrin function in maintenance of sarcomeres during muscle contraction. To distinguish between these possibilities, we tested whether the *unc-70* phenotype was suppressed by *unc-54(e1092)*. *unc-54* encodes the predominant myosin in the body muscles, and *unc-54* mutant animals are capable of only weak muscle contractions (Dibb et al., 1985). We found that *unc-54 (e1092); unc-70(r974)* animals were significantly longer than *unc-70(r974)* animals, although not as long as the wild type (Fig. 10). These data indicate that muscle contraction causes at least part of the length defect in *unc-70*, and suggest that an important function of β-spectrin in muscle is during muscle contraction.

Discussion

The results presented in this study are the first characterization of adult animals lacking β-spectrin, a component of the membrane skeleton that is found in most tissues in vertebrates and *C. elegans*. The *unc-70* gene encodes the *C. elegans* homologue of β-spectrin. Animals homozygous for null alleles of *unc-70* that have been previously characterized as lethal mutations can survive and propagate under certain conditions. These animals have two striking phenotypes: they are paralyzed and dumpy. To determine which cellular processes are disrupted in *unc-70* animals, we examined three tissues in which β-spectrin is expressed: gut epithelia, neurons, and muscles.

In erythrocytes and in some other tissues, the loss of β-spectrin leads to general defects of the plasma membrane such as herniation and the loss of cell adhesion (for review see Lux and Palek, 1995). Thus, one possible func-

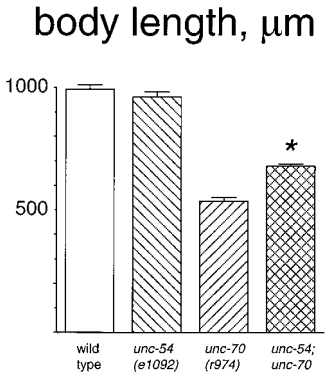

Figure 10. Suppression of *unc-70* length defects by a mutation in the body wall myosin. Adult progeny of homozygous animals were mounted in 10 mM sodium azide and photographed. Length at the midline was measured using NIH Image. Wild type = 994 ± 17 μm, n = 5; *unc-54(e1092)* = 961 ± 21 μm, n = 5; *unc-70(r974)* = 536 ± 17 μm, n = 5; and *unc-54(e1092); unc-70(r974)* = 680 ± 10 μm, n = 5. *unc-54(e1092); unc-70(r974)* is significantly different from *unc-70(r974)* and from the wild type ($P < 0.001$).

tion for β-spectrin is to support general membrane integrity and adhesion. However, we did not observe any general membrane defects in *unc-70* animals. Plasma membranes and cell–cell contacts appeared normal in muscles and gut epithelia. In neurons, we also failed to observe any general membrane defects, although the defect we observed in axonal architecture could be due to membrane defects in growth cones. We conclude that *C. elegans* β-spectrin is not required for general membrane integrity or for cell adhesion.

β-Spectrin displays a differential localization in some polarized cells, such as MDCK cells and vertebrate neurons (for review see Morrow et al., 1997). This suggests that β-spectrin may be a determinant of cell polarity. However, we observed no polarity defects in any of the tissues we analyzed. In the gut epithelia, the apical and basolateral domains retained their normal identity in *unc-70* animals by a number of ultrastructural criteria. In muscles, we found the myofilament lattice to be polarized to the lateral surface and correctly oriented relative to the body axis in *unc-70* animals. In neurons, we found that the ultrastructure of neuromuscular junctions of *unc-70* animals was normal. Together, these data suggest that β-spectrin is not a determinant of cell polarity in *C. elegans*.

Although we failed to find evidence for β-spectrin function in processes of cell polarity, we did find abundant defects in *unc-70* animals, which indicate that β-spectrin is essential for specific processes at cell membranes. One process that requires β-spectrin is axon outgrowth. While *unc-70* animals appeared to have the normal complement of neurons, these neurons did not extend axons to their targets. These data suggest that β-spectrin is required in growth cones during axon extension. A role for spectrin in growth cone function is supported by the observed distribution of spectrin in cultured vertebrate neurons (Sobue and Kanda, 1989; Sobue, 1990). In these cells, spectrin is found localized to the sites of membrane–substratum adhesion in growth cones. In addition, neurite extension in cultured neuroblastoma cells is inhibited by the injection of the NH_2-terminal β-spectrin peptides, which presumably disrupt the spectrin–actin interactions (Sihag et al., 1996). Together with our results, these data suggest that functional β-spectrin is required in growth cones during neuronal outgrowth, potentially at adhesion sites. Alternatively, β-spectrin may be required in the substrate across which growth cones migrate.

β-Spectrin is also expressed at high levels in the mature nervous system of *C. elegans*, which suggests that it plays a role in neuronal function after development is complete (Sikorski et al., 1999). However, we did not observe any defects that suggested a role for β-spectrin in mature neurons. Our results suggest that β-spectrin does not function in axonal transport or synaptic vesicle localization. We observed no decrease in synaptic vesicle number, as would be expected for a defect in axonal transport of vesicles (Hall and Hedgecock, 1991). We also observed no defects in the distribution of vesicles at the synapse, as would be expected if *unc-70* was involved in synaptic vesicle localization. It has been proposed that β-spectrin is a component of the 100-nm filaments that appear to anchor synaptic vesicles to the presynaptic density (Goodman et al., 1995). We did not directly address the presence or absence of these filaments in animals lacking β-spectrin, since it was difficult to observe them even in our wild-type sections. However, our data suggest that if β-spectrin is a component of these 100-nm filaments, then either the filaments are not required for synaptic vesicle localization at the resolution of our electron micrographs, or a compensatory mechanism exists. Finally, β-spectrin does not appear to be an essential component of the presynaptic density, since this structure appears normal in electron micrographs.

It is possible that spectrin plays a role in synaptic vesicle exocytosis, rather than in the organization of the synapse. A vertebrate β-spectrin isoform has been shown to interact with the vertebrate UNC-13 protein, which is an essential component of the presynaptic vesicle release machinery (Ohara et al., 1998; Sakaguchi et al., 1998). Mutations in the *unc-13* gene in *C. elegans* prevent synaptic vesicle fusion and result in a large accumulation of vesicles at the synapse (Richmond et al., 1999). We did not observe a statistically significant accumulation of vesicles in *unc-70*, suggesting that spectrin is not required for synaptic vesicle exocytosis. Unfortunately, a more detailed analysis of such a role is not possible because of the severe developmental defects in the *unc-70* nervous system.

In addition to its role in neuronal development, we also identified a requirement for β-spectrin in muscles. Our analysis of muscle structure in animals lacking β-spectrin demonstrated that the sarcoplasmic reticulum was absent from around the dense bodies, and that the thin filament attachment structures (dense bodies) and the thick filament attachment structures (M lines) were disrupted. β-Spectrin is specifically found at thin and thick filament attachment structures in both *C. elegans* (Moorthy et al., 2000 [this issue]) and vertebrate muscle (Nelson and Lazarides, 1984), and the regular, striated arrangement of myofilaments is blurred in *unc-70* mutant animals. These data suggest that β-spectrin may function to link the sarcoplasmic reticulum and the thin filaments to the dense bodies, and the M lines to the cell membrane. In the absence of β-spectrin, the myofilament lattice detaches from its anchors and becomes disorganized. Alternatively, β-spectrin could be playing a more direct role in muscle contraction. Specifically, we found that the dumpy phenotype of β-spectrin mutants was partially suppressed by a mutation that reduces muscle contraction. Moreover, in animals lacking β-spectrin, thick filaments invaded the I bands, suggesting that these muscles are hypercontracted. Thus, β-spectrin and the membrane skeleton may function as a compressive spring in muscle, acting to return muscle cells to their expanded state after contraction.

Our analysis of β-spectrin in *C. elegans* suggests that β-spectrin's function in nonerythrocyte cells is not for general membrane support since we observed no defects in membrane integrity in any of the tissues we examined. β-Spectrin does not appear to be essential for the generation or maintenance of cell polarity since we found no cell polarity defects in any tissue. We conclude that β-spectrin has specific but essential functions in a variety of tissues. The link that unites these functions is likely to be the membrane skeleton's ability to anchor proteins at or near the plasma membranes. While sarcomere stabilization and neuronal outgrowth appear to be dissimilar processes,

their requirement for β-spectrin suggests that muscles and neurons use a common mechanism to control protein localization at membranes, although the specific target proteins may differ.

We thank Yan Zhu for fine-mapping and cosmid rescue of *unc-70*, Ed King and Mike Bastiani for assistance with microscopy, and the members of the Jorgensen lab for helpful suggestions. *unc-70* strains were provided by P. Anderson, B.M. Cali, H.R. Horvitz, D. Baillie, and the *C. elegans* Genetics Center. *oxIs12* was a gift of K. Schuske. Y. Kohara provided the yk144e2 and yk164c6 cDNA clones. P. Okkema provided the cDNA library. Other GFP clones were obtained from A. Fire. B. Bamber contributed the worm RNA.

M. Hammarlund was supported by a National Institutes of Health Developmental Biology Training grant. This work was supported by a grant from the NIH to E.M. Jorgensen (NS34307).

Submitted: 27 January 2000
Revised: 11 March 2000
Accepted: 13 April 2000

References

Adams, M.D., S.E. Celniker, R.A. Holt, C.A. Evans, J.D. Gocayne, P.G. Amanatides, S.E. Scherer, P.W. Li, R.A. Hoskins, R.F. Galle, et al. 2000. The genome sequence of *Drosophila melanogaster*. *Science*. 287:2185–2195.

Altschul, S.F., T.L. Madden, A.A. Schaffer, J. Zhang, Z. Zhang, W. Miller, and D.J. Lipman. 1997. Gapped BLAST and PSI-BLAST: a new generation of protein database search programs. *Nucleic Acids Res.* 25:3389–3402.

Andres, A.J., and C.S. Thummel. 1994. Methods for quantitative analysis of transcription in larvae and prepupae. *Methods Cell Biol.* 44:565–573.

Bennett, V. 1990. Spectrin-based membrane skeleton: a multipotential adaptor between plasma membrane and cytoplasm. *Physiol. Rev.* 70:1029–1065.

Bennett, V., and P.J. Stenbuck. 1979. Identification and partial purification of ankyrin, the high affinity membrane attachment site for human erythrocyte spectrin. *J. Biol. Chem.* 254:2533–2541.

Bennett, V., and D.M. Gilligan. 1993. The spectrin-based membrane skeleton and micron-scale organization of the plasma membrane. *Annu. Rev. Cell Biol.* 9:27–66.

Brenner, S. 1974. The genetics of *Caenorhabditis elegans*. *Genetics*. 77:71–94.

Cali, B.M., and P. Anderson. 1998. mRNA surveillance mitigates genetic dominance in *Caenorhabditis elegans*. *Mol. Gen. Genet.* 260:176–184.

Chalfie, M., Y. Tu, G. Euskirchen, W.W. Ward, and D.C. Prasher. 1994. Green fluorescent protein as a marker for gene expression. *Science.* 263:802–805.

Clark, S.G., X. Lu, and H.R. Horvitz. 1994. The *Caenorhabditis elegans* locus *lin-15*, a negative regulator of a tyrosine kinase signaling pathway, encodes two different proteins. *Genetics*. 137:987–997.

C. elegans Sequencing Consortium. 1998. Genome sequence of the nematode *C. elegans:* a platform for investigating biology. *Science.* 282:2012–2018.

Davis, L.H., and V. Bennett. 1994. Identification of two regions of beta G spectrin that bind to distinct sites in brain membranes. *J. Biol. Chem*. 269:4409–4416.

Dibb, N.J., D.M. Brown, J. Karn, D.G. Moerman, S.L. Bolten, and R.H. Waterston. 1985. Sequence analysis of mutations that affect the synthesis, assembly and enzymatic activity of the *unc-54* myosin heavy chain of *Caenorhabditis elegans*. *J. Mol. Biol.* 183:543–551.

Drubin, D.G., and W.J. Nelson. 1996. Origins of cell polarity. *Cell*. 84:335–344.

Goh, P.Y., and T. Bogaert. 1991. Positioning and maintenance of embryonic body wall muscle attachments in *C. elegans* requires the *mup-1* gene. *Development*. 111:667–681.

Goodman, S.R., W.E. Zimmer, M.B. Clark, I.S. Zagon, J.E. Barker, and M.L. Bloom. 1995. Brain spectrin: of mice and men. *Brain Res. Bull.* 36:593–606.

Hall, D.H., and E.M. Hedgecock. 1991. Kinesin-related gene *unc-104* is required for axonal transport of synaptic vesicles in *C. elegans*. *Cell*. 65:837–847.

Hu, R.J., M. Watanabe, and V. Bennett. 1992. Characterization of human brain cDNA encoding the general isoform of beta-spectrin. *J. Biol. Chem*. 267: 18715–18722.

Johnsen, R.C., and D.L. Baillie. 1991. Genetic analysis of a major segment [LGV(left)] of the genome of *Caenorhabditis elegans*. *Genetics*. 129:735–752.

Kennedy, S.P., S.A. Weed, B.G. Forget, and J.S. Morrow. 1994. A partial structural repeat forms the heterodimer self-association site of all beta-spectrins. *J. Biol. Chem*. 269:11400–11408.

Knobel, K.M., E.M. Jorgensen, and M.J. Bastiani. 1999. Growth cones stall and collapse during axon outgrowth in *Caenorhabditis elegans*. *Development*. 126:4489–4498.

Krause, M. 1995. Techniques for analyzing transcription and translation. *Methods Cell Biol.* 48:513–529.

Lee, J.K., E. Brandin, D. Branton, and L.S. Goldstein. 1997. alpha-Spectrin is required for ovarian follicle monolayer integrity in *Drosophila melanogaster*. *Development*. 124:353–362.

Lux, S.E., and J. Palek. 1995. Disorders of the red cell membrane. *In* Blood: Principles and Practice of Hematology. R.I. Handin, S.E. Lux, and T.P. Stossel, editors. J.B. Lippincott Company, Philadelphia. 1701–1818.

McIntire, S.L., E. Jorgensen, J. Kaplan, and H.R. Horvitz. 1993. The GABAergic nervous system of *Caenorhabditis elegans*. *Nature*. 364:337–341.

McIntire, S.L., R.J. Reimer, K. Schuske, R.H. Edwards, and E.M. Jorgensen. 1997. Identification and characterization of the vesicular GABA transporter. *Nature*. 389:870–876.

McKeown, C., V. Praitis, and J. Austin. 1998. *sma-1* encodes a betaH-spectrin homolog required for *Caenorhabditis elegans* morphogenesis. *Development*. 125:2087–2098.

Mello, C.C., J.M. Kramer, D. Stinchcomb, and V. Ambros. 1991. Efficient gene transfer in *C. elegans*: extrachromosomal maintenance and integration of transforming sequences. *EMBO (Eur. Mol. Biol. Organ.) J.* 10:3959–3970.

Miller, D.M., and D.C. Shakes. 1995. Immunofluorescence microscopy. *Methods Cell Biol.* 48:365–394.

Moorthy, S., L. Chen, and V. Bennett. 2000. *C. elegans* βG-spectrin is dispensable for establishment of epithelial polarity but is essential for muscular and neuronal function. *J. Cell Biol.* 149:915–930.

Morrow, J., D. Rimm, S. Kennedy, C. Cianci, J. Sinard, and S. Weed. 1997. Of membrane stability and mosaics: the spectrin cytoskeleton. *In* Handbook of Physiology, Cell Physiology. 485–540.

Nelson, W.J., and E. Lazarides. 1984. Goblin (ankyrin) in striated muscle: identification of the potential membrane receptor for erythroid spectrin in muscle cells. *Proc. Natl. Acad. Sci. USA*. 81:3292–3296.

Nelson, W.J., and P.J. Veshnock. 1986. Dynamics of membrane–skeleton (fodrin) organization during development of polarity in Madin-Darby canine kidney epithelial cells. *J. Cell Biol.* 103:1751–1765.

Ohara, O., R. Ohara, H. Yamakawa, D. Nakajima, and M. Nakayama. 1998. Characterization of a new beta-spectrin gene which is predominantly expressed in brain. *Brain Res. Mol. Brain Res.* 57:181–192.

Park, E.C., and H.R. Horvitz. 1986. Mutations with dominant effects on the behavior and morphology of the nematode *Caenorhabditis elegans*. *Genetics*. 113:821–852.

Porter, G.A., G.M. Dmytrenko, J.C. Winkelmann, and R.J. Bloch. 1992. Dystrophin colocalizes with β-spectrin in distinct subsarcolemmal domains in mammalian skeletal muscle. *J. Cell Biol.* 117:997–1005.

Richmond, J.E., W.S. Davis, and E.M. Jorgensen. 1999. UNC-13 is required for synaptic vesicle fusion in *C. elegans*. *Nat. Neurosci.* 2:959–964.

Sakaguchi, G., S. Orita, A. Naito, M. Maeda, H. Igarashi, T. Sasaki, and Y. Takai. 1998. A novel brain-specific isoform of beta spectrin: isolation and its interaction with Munc13. *Biochem. Biophys. Res. Commun.* 248:846–851.

Sihag, R.K., T.B. Shea, and F.S. Wang. 1996. Spectrin-actin interaction is required for neurite extension in NB 2a/dl neuroblastoma cells. *J. Neurosci. Res.* 44:430–437.

Sikorski, A.F., J. Sangerman, S.R. Goodman, and S.D. Critz. 1999. Spectrin (βSpIIΣ1) is an essential component of synaptic transmission. *Brain Res.* 852:161–166.

Sobue, K. 1990. Involvement of the membrane cytoskeletal proteins and the src gene product in growth cone adhesion and movement. *Neurosci. Res. Suppl.* 13:S80–S91.

Sobue, K., and K. Kanda. 1989. Alpha-actinins, calspectin (brain spectrin or fodrin), and actin participate in adhesion and movement of growth cones. *Neuron*. 3:311–319.

Thomas, G.H., and D.P. Kiehart. 1994. Beta heavy-spectrin has a restricted tissue and subcellular distribution during *Drosophila* embryogenesis. *Development*. 120:2039–2050.

Thomas, G.H., D.C. Zarnescu, A.E. Juedes, M.A. Bales, A. Londergan, C.C. Korte, and D.P. Kiehart. 1998. *Drosophila* betaHeavy-spectrin is essential for development and contributes to specific cell fates in the eye. *Development*. 125:2125–2134.

Thompson, J.D., D.G. Higgins, and T.J. Gibson. 1994. CLUSTAL W: improving the sensitivity of progressive multiple sequence alignment through sequence weighting, position-specific gap penalties and weight matrix choice. *Nucleic Acids Res.* 22:4673–4680.

White, J. 1988. The anatomy. W.B. Wood, editor. *In* The Nematode *Caenorhabditis elegans*. Cold Spring Harbor Laboratory Press, Cold Spring Harbor, NY. 81–122.

White, J.G., E. Southgate, J.N. Thomson, and S. Brenner. 1986. The structure of the nervous system of the nematode *Caenorhabditis elegans*. *Phil. Trans. R. Soc. Lond*. 314:1–340.

Yan, Y., E. Winograd, A. Viel, T. Cronin, S.C. Harrison, and D. Branton. 1993. Crystal structure of the repetitive segments of spectrin. *Science*. 262:2027–2030.

Zhou, D., J.A. Ursitti, and R.J. Bloch. 1998. Developmental expression of spectrins in rat skeletal muscle. *Mol. Biol. Cell*. 9:47–61.